A Comparative Study of Some Spatial-temporal Discretization Schemes for Nonlinear Magnetohydrodynamic Simulation of Plasmas

D. Nath, M. S. Kalra* and P. Munshi
Nuclear Engineering and Technology Program
Indian Institute of Technology Kanpur
Kanpur - 208 016 India
(dnath@iitk.ac.in, *msk@iitk.ac.in, pmunshi@iitk.ac.in)

Abstract

A large number of numerical schemes have been developed for the integration of the hyperbolic system of partial differential equations (PDEs) arising in the magnetohydrodynamic (MHD) simulation of plasmas. These schemes can be based on either the combined space and time discretization such as the Lax-Wendroff type schemes, or one may perform first a separate space discretization leading to a semidiscretized set of ordinary differential equations (ODEs), which are then separately integrated in time. In this work, a comparative study of two schemes based on simultaneous discretization of space and time (Richtmyer two-step Lax-Wendroff scheme and MacCormack scheme) and one scheme based on centered-space semidiscretization followed by time integration by the fourth-order Runge-Kutta method, is presented. Particular attention is paid to the applicability of the *linear* stability criteria to the numerical integration of *nonlinear* MHD equations with geometry and field components of a linear θ-pinch.

1. Introduction

High-temperature magnetized fusion plasmas such as exist in tokomaks or other modern magnetic fusion devices can be described using kinetic or fluid models. However, the wide range of time and space scales present in the kinetic description of plasmas make numerical simulation based on kinetic equation extremely difficult. As a result, fluid models, particularly the magnetohyrodynamic (MHD) or the extended MHD models, are extensively used in the numerical simulation of tokomak and other magnetized plasmas. These models adequately describe a large number of phenomena of interest in magnetic fusion.

The MHD model of the magnetic fusion plasma results in a system of *nonlinear hyperbolic equations*. Numerical solution of even these reduced systems of equations poses a challenge because there are multiple conserved quantities and multiple characteristic speeds. Even a single *linear* advection equation with a constant characteristic velocity is not amenable to straightforward numerical integration and requires a careful consideration of stability condition and errors resulting from numerical diffusion and dispersion. For example, the most straightforward finite difference method, the forward–time centered-space (FTCS) method, which is conditionally stable when applied to the diffusion equation turns out to be unconditionally unstable for the advection equation [1,2]. In this work we present a comparative study of some of the spatial-temporal discretization schemes which are in use for the numerical integration of the hyperbolic system of partial differential equations arising in

the MHD models of magnetized fusion plasmas. These are briefly described in the remainder of introduction.

A modification of the FTCS method proposed by Lax and known as Lax-Friedrichs scheme is conditionally stable but suffers from excessive numerical damping. It is of first order accuracy in time and its truncation error becomes unbounded as time step tends to zero for a fixed spatial grid. For this reason, it is not regarded as a consistent approximation to the advection problem [2,3] and has not been used in this work. Instead, a two-step Lax-Wendroff type method developed by Richtmyer, and a predictor-corrector Lax-Wendroff type method developed by MacCormack [3,4], is used. Both these methods use simultaneous discretization of space and time and can be readily applied to systems of nonlinear hyperbolic equations, although, as is shown later, the linear stability criterion based on Courant-Friedrichs-Levy (CFL) condition, turns out to be only a necessary and not a sufficient condition for the stability of numerical simulations of the nonlinear problem. In addition to the two numerical schemes mentioned above, one scheme based on the *method of lines*, also known as semidiscretisation [4,5] is also considered in this work. The resulting system of ODEs is then solved by the fourth-order Runge-Kutta method [3,6].

In what follows, the mathematical formulation of the problem to which these methods are applied and compared, is presented. Applicability of the linear stability criteria is examined by direct numerical simulation of the nonlinear problem. Numerical diffusion and dispersion errors are assessed from the numerical amplification factor based on the local Courant number (CFL condition).

2. Governing Equations

For a comparative study of three spatiotemporal discretization schemes discussed above, a one-dimensional cylindrical geometry with magnetic field and plasma current components as shown in Figure 1 is chosen. Time dependent one dimensional ideal MHD equations for this configuration can be written as [7−9].

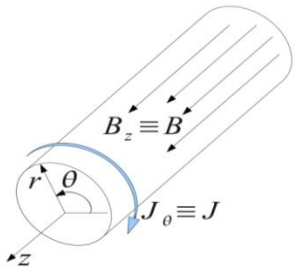

Figure 1 Schematic diagram of the linear θ-pinch configuration

$$\begin{aligned}
\frac{\partial \rho}{\partial t} &= -\frac{1}{r}\frac{\partial}{\partial r}(r\rho v),\\
\frac{\partial v}{\partial t} &= -v\frac{\partial v}{\partial r} - \frac{1}{\rho}\frac{\partial}{\partial r}\left(P + \frac{B^2}{2\mu_0}\right),\\
\frac{\partial P}{\partial t} &= -v\frac{\partial P}{\partial r} - \gamma\frac{P}{r}\frac{\partial}{\partial r}(rv),\\
\frac{\partial B}{\partial t} &= -\frac{B}{r}\frac{\partial}{\partial r}(rv) - v\frac{\partial B}{\partial r},
\end{aligned} \tag{1}$$

where symbols are explained in the Nomenclature.

Nondimensionalization

The following transformations are used to write the above equations in a dimensionless form:

$$r \to ra, \qquad t \to \frac{ta}{v_A}, \qquad \rho \to \rho\rho_0, \qquad v \to vv_A, \qquad P \to PP_0, \qquad B \to BB_a;$$

where $v_A = \sqrt{(B_a^2/\mu_0\rho_0)}$ is the Alfvén speed and other symbols are given in the Nomenclature. Using these transformations, Eqs. (1) can be written in the following dimensionless form:

$$\begin{aligned}
\frac{\partial \rho}{\partial t} &= -\frac{1}{r}\frac{\partial}{\partial r}(r\rho v), \\
\frac{\partial v}{\partial t} &= -v\frac{\partial v}{\partial r} - \frac{\beta}{2}\frac{1}{\rho}\frac{\partial}{\partial r}\left(P + \frac{B^2}{\beta}\right), \\
\frac{\partial P}{\partial t} &= -v\frac{\partial P}{\partial r} - \gamma\frac{P}{r}\frac{\partial}{\partial r}(rv), \\
\frac{\partial B}{\partial t} &= -\frac{B}{r}\frac{\partial}{\partial r}(rv) - v\frac{\partial B}{\partial r},
\end{aligned} \tag{2}$$

where $\beta = P_0/(B_a^2/2\mu_0)$. The above equations can be written in the following matrix form

$$\frac{\partial \mathbf{U}}{\partial t} + \mathbf{A}(\mathbf{U})\frac{\partial \mathbf{U}}{\partial r} = \boldsymbol{S}(\mathbf{U}, r), \tag{3}$$

where,

$$\mathbf{U} = \begin{Bmatrix} \rho \\ v \\ P \\ B \end{Bmatrix}, \qquad \mathbf{A}(\mathbf{U}) = \begin{bmatrix} v & \rho & 0 & 0 \\ 0 & v & \beta/2\rho & B/\rho \\ 0 & \gamma P & v & 0 \\ 0 & B & 0 & v \end{bmatrix}, \qquad \mathbf{S}(\mathbf{U}, r) = \begin{Bmatrix} -\rho v/r \\ 0 \\ -\gamma v P/r \\ -vB/r \end{Bmatrix}. \tag{4}$$

3. Initial and Boundary Conditions

The system of Eqs. (2) or (3) can be solved numerically starting from any initial condition of the plasma and applying appropriate boundary conditions. For the simulations carried out in the present work, we start with a stationary (quiescent) equilibrium state of the plasma and introduce an initial disturbance (not necessarily small). The temporal evolution of the plasma is then studied both in its transient phase and the final steady state using various schemes within their (linear) stability regimes. The system of Eqs. (2) or (3) has a wide variety of confined equilibria in which the pressure is peaked at the center and monotonically decreases to zero at the edge [8]. The azimuthal current, and therefore pressure gradient, must be zero at $r = 0$ and also at $r = 1$ if $P = 0$ at $r = 1$. Here, the simplest algebraic profile for the

dimensionless P in terms of the dimensionless radius which satisfies these conditions is chosen:

$$P(r,0) = 1 - 3r^2 + 2r^3; \qquad 0 \le r \le 1, \tag{5}$$

and corresponding initial profile for the dimensionless magnetic field is given by

$$B(r,0) = \sqrt{1 - \beta(1 - 3r^2 + 2r^3)}; \qquad 0 \le r \le 1. \tag{6}$$

The initial density profile can be chosen independently, each choice corresponding to a different temperature profile. Since our purpose in the present work is only to study the applicability and stability of the various numerical algorithms, an initial density profile same as initial pressure profile is used implying an isothermal plasma. For the numerical results presented here, a sinusoidal disturbance is introduced in the equilibrium pressure distribution changing the initial pressure distribution to

$$P(r,0) = (1 - 3r^2 + 2r^3)[1 + \delta \sin(2\pi r)]; \qquad 0 \le r \le 1. \tag{7}$$

This disturbed initial pressure profile respects all the boundary conditions at $r = 0$ and $r = 1$. The boundary conditions for all the state variables are given below:

$$\begin{array}{lllll} \text{At} \quad r = 0, & \dfrac{\partial \rho}{\partial r} = 0, & v = 0, & \dfrac{\partial P}{\partial r} = 0, & \dfrac{\partial B}{\partial r} = 0; \\ \text{at} \quad r = 1, & \rho = 0, & v = 0, & P = 0, & B = 1. \end{array} \tag{8}$$

It may be stated here that any other set of initial and boundary conditions can be chosen which may be relevant for a given plasma. The numerical results presented later are with the initial and boundary conditions as stated above. The parameter δ in the disturbed pressure profile, Eq. (7), is taken as equal to 0.1 for all simulations.

4. The Linear Stability Conditions

It can be easily seen that the eigenvalues, λ, of the matrix **A** in Eq. (3) are real for all physically acceptable values of **U**, confirming that this system of equations is pure hyperbolic. It is easily ascertained that

$$\Lambda \equiv |\lambda_A|_{max} = \sqrt{\frac{B^2}{\rho} + \frac{\beta\gamma P}{2\rho}} + |v|. \tag{9}$$

The stability considerations of the numerical schemes are based on the von Neumann analysis of a scalar linear advection equation with advection speed equal to the characteristic speed Λ [2,3]:

$$\frac{\partial u}{\partial t} + \Lambda \frac{\partial u}{\partial r} = 0. \tag{10}$$

For a time step from $t^{(n)}$ to $t^{(n+1)}$, the *numerical amplification factor*, G, which is complex in general, is given by:

$$\mathrm{G} = \frac{u^{n+1}}{u^n}. \tag{11}$$

The modulus of G provides a measure of numerical dissipation or damping and must be less than unity for the stability of the numerical algorithm. The phase of G provides a measure of numerical dispersion [1,5].

4.1 Stability condition for Lax-Wendroff-Richtmyer and MacCormack schemes

The linear stability criteria for these two schemes are identical. The amplification factor G and its modulus are given by [1−3]:

$$\mathrm{G} = (1 - \mathrm{C}^2 + \mathrm{C}^2 \cos\phi) + j(-\mathrm{C}\sin\phi); \qquad j = \sqrt{-1}$$

$$|\mathrm{G}| = \sqrt{1 - 4\mathrm{C}^2(1-\mathrm{C}^2)\sin^4(\phi/2)}. \tag{12}$$

It can be seen easily that for all values of ϕ (*dimensional mesh wave number*), $|\mathrm{G}| \leq 1$ if the Courant number,

$$\mathrm{C} = \frac{\Lambda\,\Delta t}{\Delta r} \leq 1, \tag{13}$$

where Δt is the time step and Δr grid spacing. It should be mentioned that for nonlinear problems or nonconstant matrices **A**, Λ will be different at different grid points and the stability condition must be satisfied for all grid points.

4.2 Stability condition for for the semidiscretization scheme

One of the methods used for numerical simulation in this work is based on centered-space differencing which converts the original system of PDEs, Eqs. (2) or (3), to a system of ODEs in time which are then solved by the fourth-order Runge-Kutta method. The numerical amplification factor, G, for this method is given by [3]:

$$\mathrm{G} = 1 - (\alpha\Delta t) + \frac{1}{2}(\alpha\Delta t)^2 - \frac{1}{6}(\alpha\Delta t)^3 + \frac{1}{24}(\alpha\Delta t)^4, \tag{14}$$

for a scalar linear ODE

$$\frac{du}{dt} + \alpha \mathrm{u} = 0. \tag{15}$$

If in the advection equation, Eq. (10), centered-space differencing is used, it is straightforward to see that the amplification factor for the advection equation is obtained by the following replacement for $\alpha\Delta t$ in Eq. (14):

$$\alpha\Delta\mathrm{t} = \frac{\Lambda\,\Delta t}{2\Delta r}\left(e^{j\phi} - e^{-j\phi}\right) = \frac{\Lambda\,\Delta t}{2\Delta r} j sin\phi = \mathrm{C} j sin\phi.$$

This yields:

$$\mathrm{G} = \left(1 - \tfrac{1}{2}\mathrm{C}^2\sin^2\phi + \tfrac{1}{24}\mathrm{C}^4\sin^4\phi\right) + j\left(-\mathrm{C}\sin\phi + \tfrac{1}{6}\mathrm{C}^3\sin^3\phi\right),$$
$$|\mathrm{G}| = \sqrt{1 - \tfrac{1}{72}\mathrm{C}^6\left(1 - \tfrac{1}{8}\mathrm{C}^2\sin^2\phi\right)\sin^6\phi}. \qquad (16)$$

It is easy to see that $|\mathrm{G}| \leq 1$ if

$$\mathrm{C} = \frac{\Lambda\,\Delta t}{\Delta r} \leq 2\sqrt{2}, \qquad (17)$$

which coincides with the stability criterion obtained in [5] by the *matrix method of stability analysis* for the fourth order Runge-Kutta method applied to semidiscretized schemes.

5. Numerical Results and Discussion

Results of numerical simulations of Eqs. (2), subject to initial and boundary conditions given in Eqs. (6−8), using the three schemes are given in Figures (2−10). In these figures, the Lax-Wendroff-Richtmyer two-step scheme is designated as LWR, the MacCormack scheme is designated as MAC, and the scheme based on centered-space semidiscretization followed by time integration by the fourth-order Runge-Kutta method is designated as RK4. It may be mentioned here that the MacCormack scheme can be implemented in three versions [1,4], which give nearly identical results (for the problem studied here). We have implemented the symmetric version which alternates the forward and backward differencing in the predictor and corrector between successive time steps. In all the numerical simulations, the linear stability criteria are satisfied, with Courant number, $\mathrm{C} \leq 0.8$ at the center of all grid points.

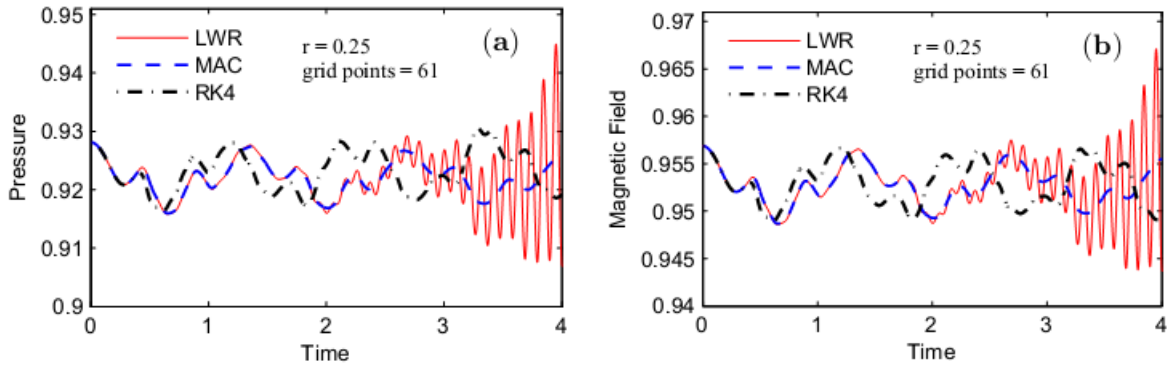

Figure 2 Comparison of numerical solution of Eqs. (2) by different schemes(a) dimensionless pressure and (b) dimensionless magnetic field at $r = 0.25$ and grid points $= 61$.

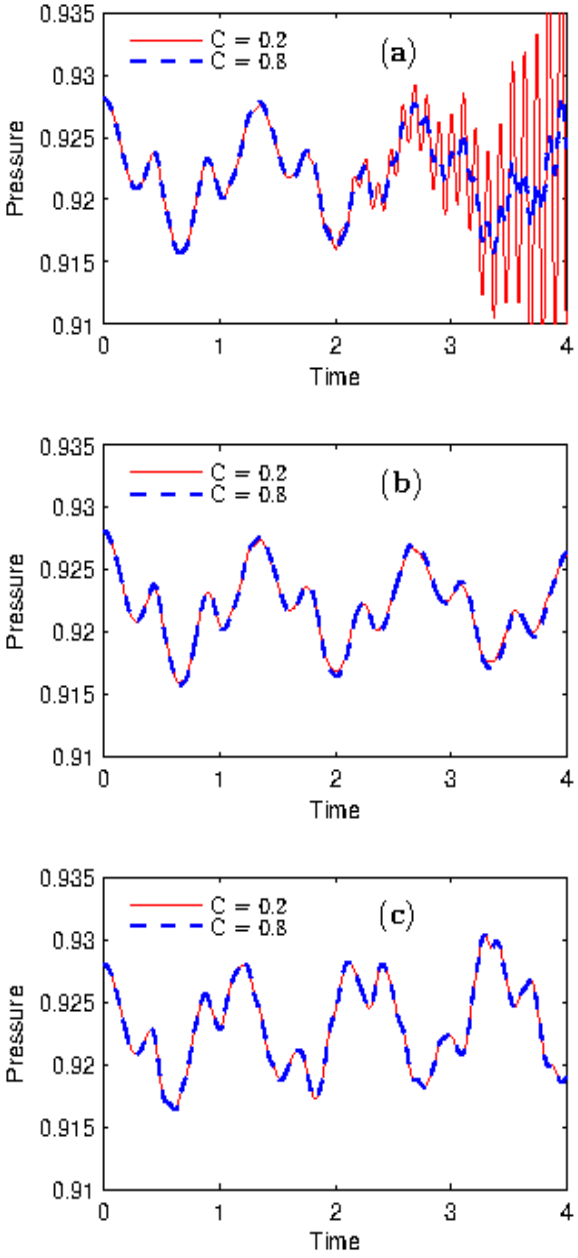

Figure 3 Effect of Courant number in:
(a) Lax-Wendroff-Richtmyer scheme,
(b) MacCormack scheme and
(c) fourth-order Runge-Kutta scheme.

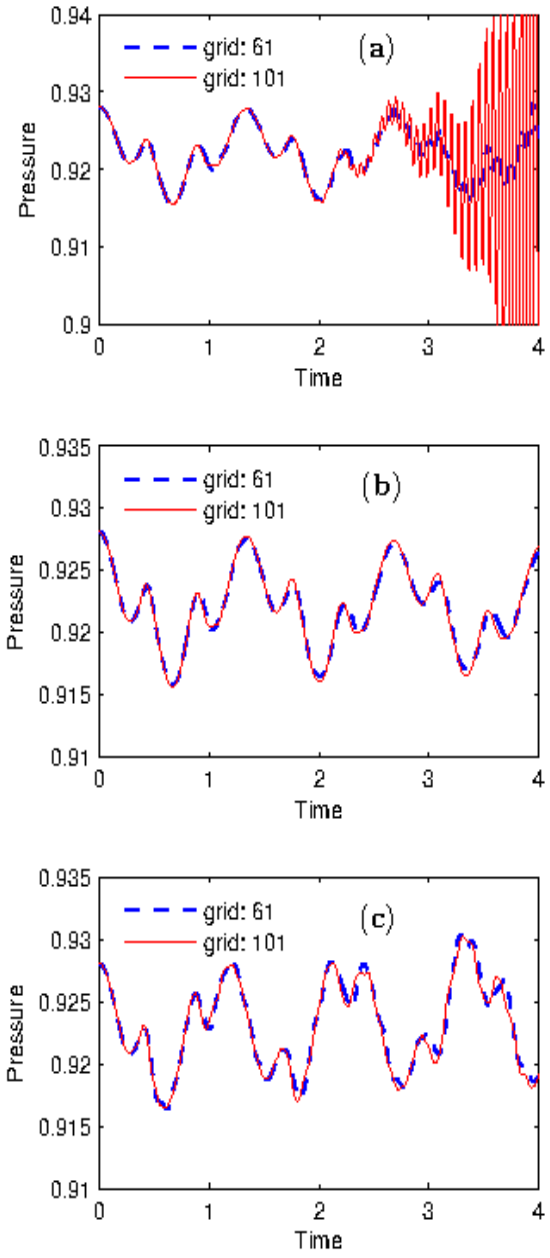

Figure 4 Effect of grid refinement with fixed Courant number C = 0.8:
(a) Lax-Wendroff-Richtmyer scheme,
(b) MacCormack scheme and
(c) fourth-order Runge-Kutta scheme.

Figures (2−4) show results of simulations upto dimensionless time $t = 4$, i.e., upto four-times the time it takes Alfvén waves to cross the plasma (minor) radius. The significant differences

in the results obtained by the three schemes are apparent in Figure 2a and 2b. The effect of the Courant number is shown in Figures (3a−3c), and is found to be particularly pronounced for the LWR scheme (Figure 3a). The effect of grid refinement, while keeping the Courant number same, on the three schemes is shown in Figures (4a−4c). It can be seen in Figure 4a that the linear stability condition is not always sufficient for ensuring the numerical stability when simulating a nonlinear problem. This is particularly true for the LWR scheme, Figure 4a, but also true for RK4, Figure 4c, where the instability builds slowly for all cases, even when the linear stability condition is satisfied. On the other hand, the MacCormack scheme gives numerically stable results if the linear stability condition is satisfied. *This is true for the nonlinear problem solved in this work and may not be true when applied to other nonlinear problems.*

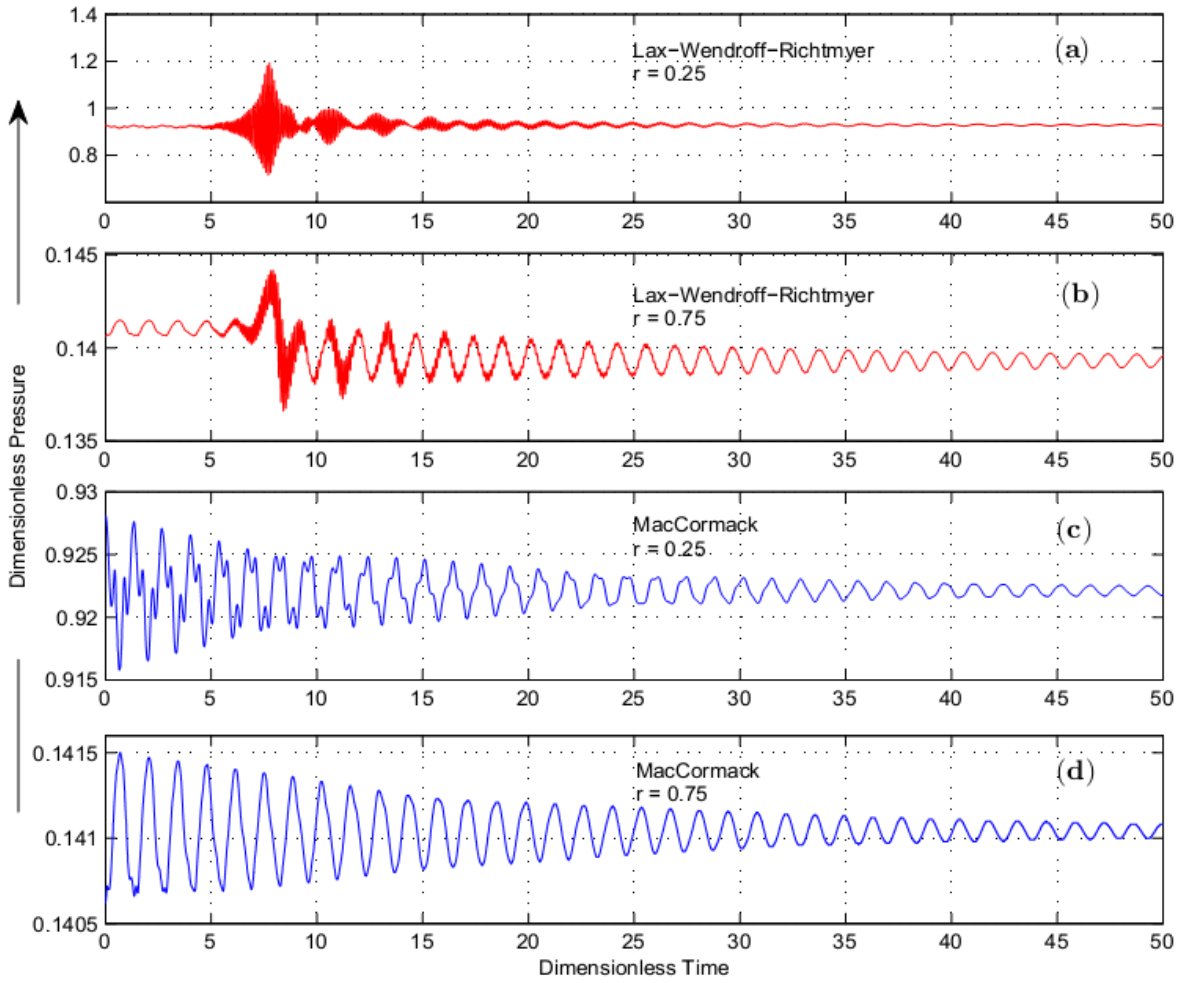

Figure 5 Time evolution of dimensionless in Eqs. (2) upto t = 50 for Lax-Wendroff-Richtmyer and MacCormack schemes at the radial distances $r = 0.25$ and $r = 0.75$.

Figure 5 gives time evolution using MAC and LWR schemes. The quasi-steady state solutions obtained at $t = 50$ by the two schemes compare well as shown in Figure 6. As mentioned

above, LWR scheme does not always give stable results, even when the linear stability criterion is satisfied. However, in those cases where it remains stable, the results match well with the MAC scheme, except during the initial transient phase. Long time results using RK4 are not shown as the scheme invariably builds upto an instability, even when linear stability criterion is satisfied. As mentioned later, this may be due to the negligible numerical dissipation or insufficiency of the linear stability criterion for the nonlinear problem.

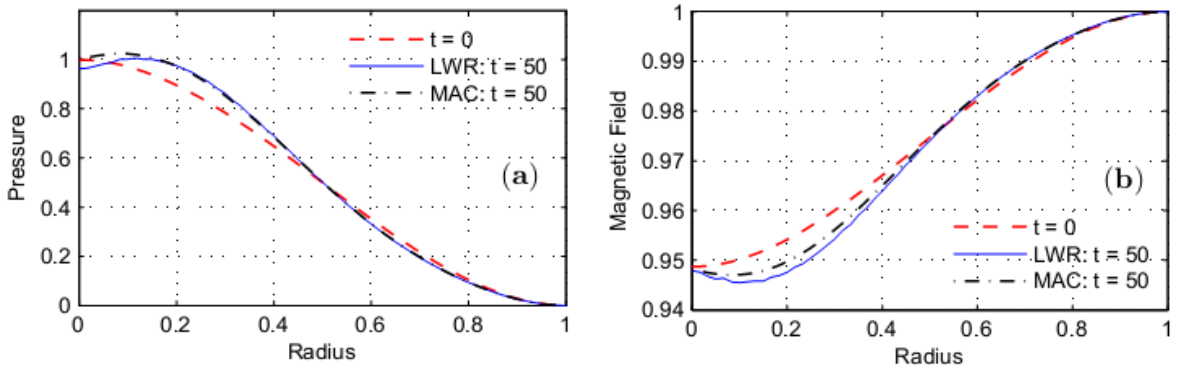

Figure 6 Radial distribution of (a) pressure, (b) magnetic field for two schemes Lax-Wendroff-Richtmyer and MacCormack at t = 0 and t = 50.

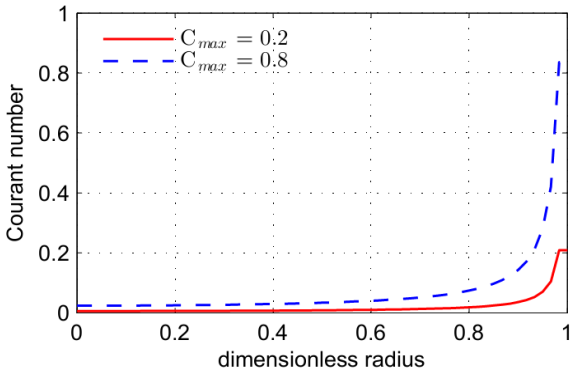

Figure 7 Radial variation of Courant number. The maximum value of Courant number, at the edge ($r = 1$), is $C = 0.8$ for Lax-Wendroff-Richtmyer scheme and $C = 0.2$ for MacCormack scheme.

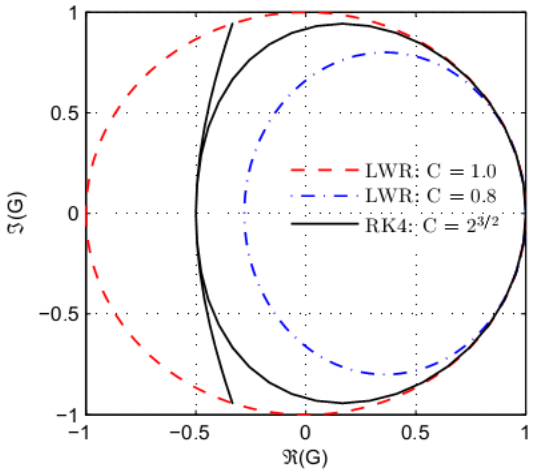

Figure 8 Numerical amplification factor, G, in the complex plane.

Figure 7 shows the variation of the Courant number across the (dimensionless) radius of the plasma. It can be seen that if the condition $C \leq 1$ is satisfied at the center of outermost grid interval, it is satisfied at all other points of the grid. Figure 8 shows that if the conditions in Eq. (13) and (17) are satisfied, the respective plots of the numerical amplification factor lie

within the unit circle on the complex plane, implying $|G| \leq 1$. This can also be seen in Figures 9a and 10a, where $|G|$ is plotted as a function of dimensional *mesh wave number* ϕ in the range $-\pi$ to π.

Finally, Figures 9b and 10b show the dispersion or phase error. A positive dispersion error implies that numerical advection velocity is larger than the exact physical velocity. The differences observed in the numerical results obtained using the three schemes are due to different numerical dissipation and dispersion introduced by each scheme. In particular, there is very little numerical dissipation in RK4, Figure 10a, where it can be observed that $|G| \geq 0.99$. The slowly building instability (for the nonlinear problem) observed in RK4 may be due to negligible numerical dissipation.

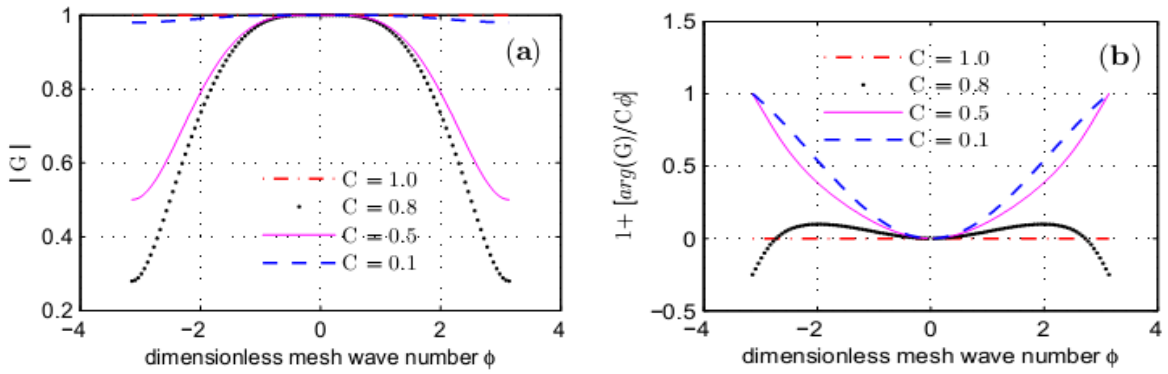

Figure 9 (a) Numerical amplification and (b) phase error for the Lax-Wendroff-Richtmyer scheme for various Courant numbers

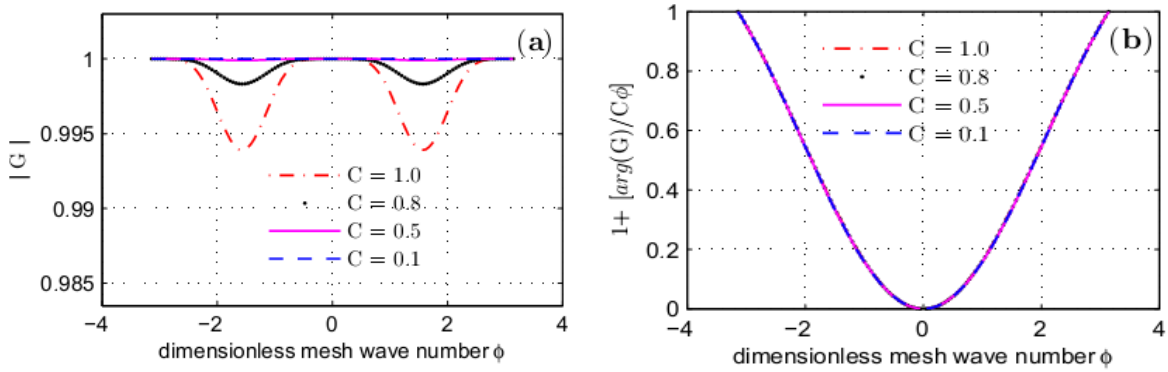

Figure 10 (a) Numerical dissipation factor and (b) phase error for the Runge-Kutta fourth order scheme for various Courant numbers.

6 Conclusion

Three widely used discretization schemes for the numerical solution of a hyperbolic system of equations are applied to a representative *nonlinear* problem arising in the magnetohydrodynamic simulation of plasmas. These include two schemes based on simultaneous discretization of space and time (the Ritchmyer two-step Lax-Wendroff scheme and the MacCormack predictor-corrector scheme with alternating forward and backward differencing between successive time steps). The third scheme used in this work consists of centered-space differencing to convert the original system of PDEs to a larger system of ODEs which are then integrated in time by the fourth order Runge-Kutta method. The linear stability criteria for these schemes are presented. Numerical simulations show that the linear stability conditions are necessary but not sufficient to guarantee the numerical stability of these algorithms when applied to a *nonlinear* hyperbolic problem. For the problem studied here, the MacCormack scheme always gave stable results. The stability of the Lax-Wendroff-Richtmyer scheme was found not to be characterized by the Courant number alone. However, in those cases where it remains stable, the long time quasi-steady state results match well with those obtained with the MacCormack scheme. The centered-space semidiscritization scheme followed by time integration by the fourth-order Runge-Kutta method developed a slowly building instability in all cases. This may be due to negligible amount of numerical damping in this scheme. The solution for the transient phase obtained from the three schemes are found to differ significantly due to different amount of numerical diffusion and dispersion present in each scheme.

Nomenclature

a	plasma minor radius	v_A	Alfvén speed
$\mathbf{A}$	coefficient matrix	α	a constant in Eq. (15)
B	magnetic field	β	normalized plasma pressure $(= 0.1)$
B_a	magnetic field at the boundary	γ	ratio of specific heats $(= 5/3)$
C	Courant number	δ	a constant $(= 0.1)$
G	numerical amplification factor	θ	azimuthal coordinate
P	pressure	λ	eigenvalue of matrix $\mathbf{A}$
P_0	pressure at the center	Λ	$\lvert\lambda_A\rvert_{max}$
r	radial coordinate	μ_0	magnetic permeability
t	time	ρ	density
$u, \mathbf{U}$	dependent variable(s)	ρ_0	density at the center
v	radial velocity	ϕ	dimensionless mesh wave number

7. References

[1] J.A. Trangenstein, "Numerical Solutions of Hyperbolic Partial Differential Equations", Cambridge University Press, Cambridge, 2007.

[2] S.C. Jardin, "Computational Methods in Plasma Physics", Taylor and Francis, Boca Raton, 2010.

[3] J.D. Hoffman, "Numerical Methods for Scientists and Engineers", McGraw-Hill, Inc., New York, 1982.

[4] J. P. Goedbloed, R. Keppens and S. Poedts, "Advanced Magnetohydrodynamics: With Applications to Laboratory and Astrophysical Plasmas", Cambridge University Press, Cambridge, 2010.

[5] C. Hirsch, "Numerical Computation of Internal and External Flows, Volume 1, Fundamentals of Numerical Discretization", John Wiley, 1989.

[6] W.H. Press, S.A. Teukolsky, W.T. Vellerling and B.P. Flannery, "Numerical Recipes in Fortran 77", Cambridge University Press, 1992.

[7] J.P. Freidberg, "Ideal Magnetohydrodynamics", Plenum Press, New York, 1982.

[8] J.P. Freidberg, "Plasma Physics and Fusion Energy", Cambridge University Press, Cambridge, 2007.

[9] R.D. Hazeltine and J.D. Meiss, "Plasma Confinement", Dover Publication, New York, 2003.